

Ionic Liquid Assisted Solvothermal Synthesis of Cu Polyhedron-Pattern Nanostructures and Their Application as Enhanced Nanoelectrocatalysts for Glucose Detection

Li Xu,^[a] Jiexiang Xia,^[a] Huaming Li,^{*[a]} Henan Li,^[a] Kun Wang,^[a] and Sheng Yin^[a]

Keywords: Copper / Ionic liquids / Solvothermal synthesis / Nanostructures / Non-enzymatic electrocatalysis

Cu polyhedron-pattern nanostructures have been successfully synthesized in the presence of the ionic liquid (IL) 1-hexadecyl-3-methylimidazolium bromide ([C₁₆mim]Br) under solvothermal conditions. The as-prepared samples were characterized by X-ray diffraction (XRD), high-resolution transmission electron microscopy (HRTEM), Fourier transform infrared (FTIR) spectroscopy and diffuse reflectance spectroscopy (DRS). During the reaction process, the ionic liquid played an important role in controlling the morphology and size of the Cu polyhedron-pattern nanostructures. The results of FTIR spectroscopic analysis indicated that there was the ionic liquid [C₁₆mim]Br on the surface of the Cu polyhedron-pattern nanostructures. Cu polyhedron-pattern nanostructures exhibited better thermal stability in air than

Cu samples synthesized without ionic liquid at room temperature. In addition, the electrocatalytic activity of the Cu-modified electrodes towards glucose oxidation was investigated by cyclic voltammetry. The results clearly demonstrated that the unique morphology and small size of the Cu polyhedron-pattern nanostructures made them suitable for application as non-enzymatic glucose sensors. Simultaneously, the [C₁₆mim]Br ionic liquid on the surface of the Cu polyhedron-pattern nanostructures had a significant impact on the electrocatalytic activity of Cu polyhedron-pattern nanostructures. Thus, electrodes modified with these Cu polyhedron-pattern nanostructures are promising for the future development of non-enzymatic glucose sensors.

1. Introduction

In the past few decades, nanomaterials have sparked great interest in the scientific world. It has been found that the characteristics of these tiny isolated materials are completely different from those of their bulk counterparts, in many cases better.^[1] Amongst the different nanomaterials, copper nanomaterials have also received considerable attention for their unusual properties and potential applications in diverse fields. The various procedures for their synthesis include microemulsion techniques,^[2] electrochemical methods,^[3] reduction of aqueous copper salts,^[4] UV-light irradiation,^[5] sonochemical methods,^[6] physical vapor deposition,^[7] and so on. The chemical reduction method has been most extensively used because of its simplicity, low cost, and the ease of controlling the size and shape of the copper nanoparticles.^[8] However, the synthesis and technological application of nanoparticles present challenges because of the tendency of the particles to agglomerate and their instability in air.^[9] To minimize copper oxidation, previous syntheses have typically been performed in nonaqueous solvents, at low precursor concentrations, and under the pro-

tection of an inert gas.^[10] Cu nanoparticles also tend to aggregate during the synthesis. Thus, a selective synthetic route for high-purity metallic Cu nanoparticles is highly desired.

In recent years, room temperature ionic liquids (RTILs) have received more and more attention in the synthesis of inorganic nanomaterials such as microwave-assisted synthesis, hydrothermal synthesis, solvothermal synthesis, and ionothermal synthesis (a new synthetic method in which ionic liquids can simultaneously act as either the solvent and potential template or structure-directing agent in the synthesis of inorganic nanomaterials^[11]). RTILs possess unique physical and chemical properties such as negligible vapor pressure, wide liquid temperature range, high thermal stability, large electrochemical window, and high ionic conductivity.^[12] Up to now, a variety of metal nanomaterials have been synthesized in RTILs, including Au nanosheets, Ag, In, Co, Rh, and Ir nanoparticles, etc.^[13,14] The results of these studies showed that ionic liquids played the roles of surfactant and stabilizer in controlling the morphology and size of the materials. The synthesis of Cu in ionic liquids was rarely reported.^[15] Prashant Singh and co-workers^[15f,15g] also studied the synthesis of the copper nanoparticles by NaBH₄ reduction in the presence of ionic liquid, and copper nanoparticles in ionic liquids have also been employed as recyclable catalysts for coupling reactions in excellent yields and with short reaction times. However,

[a] School of Chemistry and Chemical Engineering, Jiangsu University, Zhenjiang 212013, P. R. China
E-mail: lihm@ujs.edu.cn

Supporting information for this article is available on the WWW under <http://dx.doi.org/10.1002/ejic.201001160>.

no studies have been reported on the synthesis of Cu polyhedron-pattern nanostructures in the presence of ionic liquids by the solvothermal method.

This study reports a novel synthesis of Cu polyhedron-pattern nanostructures by ethylene glycol (EG) solvothermal reduction in the presence of the ionic liquid 1-hexadecyl-3-methylimidazolium bromide ($[C_{16}mim]Br$). The nanostructures synthesized in the ionic liquid showed good nanocrystallinity, stability, and small size. In the reaction process, the ionic liquid played an important role in controlling the morphology and size of the Cu nanostructures. The results of FTIR spectroscopic analysis indicated that there was the ionic liquid $[C_{16}mim]Br$ on the surface of Cu polyhedron-pattern nanostructures. These Cu polyhedron-pattern nanostructures exhibited better thermal stability in air than Cu samples synthesized without ionic liquid at room temperature. In addition, the electrocatalytic activity of electrodes modified with Cu nanostructures towards glucose oxidation was investigated by cyclic voltammetry (CV). The present research demonstrated that the unique morphology and small size of Cu polyhedron-pattern nanostructures synthesized with ionic liquid gave them the advantage of being suitable for application as non-enzymatic glucose sensors over Cu samples synthesized without ionic liquid. The ionic liquid on the surface of the Cu polyhedron-pattern nanostructures has a significant impact on the electrocatalytic activity of those nanostructures.

2. Results and Discussion

2.1. X-ray Diffraction

The crystallinity of as-prepared samples was examined by using powder XRD measurements. Figure 1 shows the XRD pattern of the as-prepared copper nanomaterial obtained by solvothermal treatment at 160 °C for 48 h in the presence of $[C_{16}mim]Br$. All the reflection peaks can be indexed to face-centered cubic copper (JCPDS card NO. 04-0836, $a = 3.615 \text{ \AA}$). No characteristic peaks of any other phases or impurities were detected, which confirmed that the as-prepared sample obtained under the current syn-

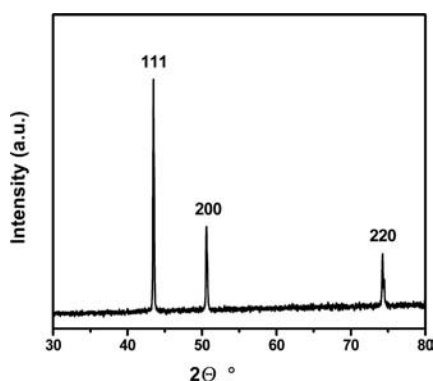


Figure 1. Typical XRD pattern of the Cu samples synthesized by solvothermal treatment at 160 °C for 48 h in the presence of $[C_{16}mim]Br$.

thetic conditions was pure Cu nanomaterial. Zhu et al.^[15e] reported that various phase ratios of CuO, Cu₂O, and Cu composite nanosheets and pure Cu nanoparticles were synthesized by hydrothermally assisted routes using ionic liquids. By contrast, it can be found that EG played the roles of solvent and reductant to reduce Cu²⁺ into Cu⁰. In addition, the as-synthesized Cu sample was also prepared in the absence of $[C_{16}mim]Br$ under the same conditions. From the preparation procedure, it was found that if the CuCl₂ solution was heated without NaOH, no precipitate would be obtained. The finding demonstrated that the reactants were not active in a non-alkali environment. Therefore, it can be concluded that the redox reaction between Cu²⁺ salt and EG can be achieved in an alkaline environment.

2.2. TEM Analysis

Figure 2 is a typical TEM image of the Cu samples obtained in different reaction systems. Cu nanostructures were observed when the solvothermal reaction was performed in the presence of $[C_{16}mim]Br$ ionic liquid (Figure 2a). Polyhedron-pattern Cu nanostructures with 20–50 nm diameter can be observed. A HRTEM image of Cu polyhedron-pattern nanostructures shown in Figure 2b reveals that the Cu samples exhibit the fivefold dissymmetry characteristic. This result suggests that Cu samples synthesized in $[C_{16}mim]Br$ ionic liquid are polyhedron-pattern nanostructures. In this picture, the crystal lattice fringes are 0.2 nm apart, which agrees with the d value of the (111) planes of the Cu crystal. For comparison, the TEM images of Cu samples synthesized without $[C_{16}mim]Br$ are shown in Figures 2c and 2d. These samples present irregular morphology with an average diameter of 1–2 μm. To sum up, as-synthesized Cu crystals prepared in the presence of the

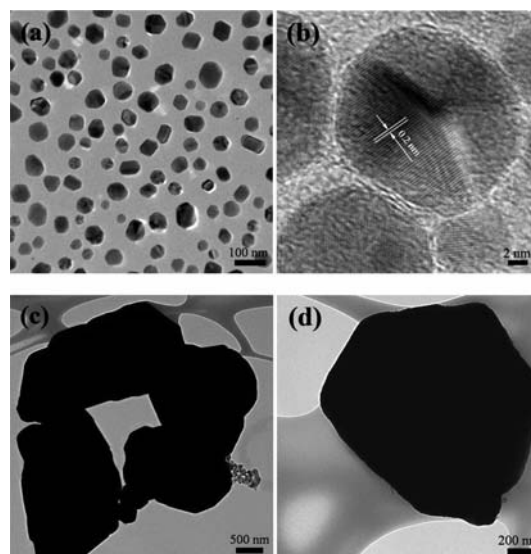


Figure 2. TEM images of Cu samples synthesized by solvothermal treatment at 160 °C for 48 h: (a) in the presence of $[C_{16}mim]Br$ ionic liquid; (c, d) in the absence of $[C_{16}mim]Br$ ionic liquid. (b) HRTEM image of Cu samples synthesized in the presence of $[C_{16}mim]Br$ ionic liquid.

ionic liquid exhibit better morphology and smaller size than Cu structures without ionic liquid. The region of the nanoparticle size could be related to the ionic liquid anion molecular volume.^[13i,13j,13k] This fact demonstrated that the ionic liquid played a crucial role in controlling the morphology and size of the Cu nanoparticles. Earlier research reported that ionic liquids acted as templates in the synthesis of inorganic nanomaterials.^[14]

2.3. FTIR Spectroscopy

Infrared spectra were used to detect the possible adsorbed species, and the FTIR spectrum of Cu polyhedron-pattern nanostructures is shown in Figure 3. The broad band centered at 3411 cm^{-1} is assigned to the O–H stretching and bending modes of water.^[16] The $\nu_{\text{C-H}}$ mode of the alkyl chain of $[\text{C}_{16}\text{mim}]^+$ is detected at 2972 cm^{-1} and 2900 cm^{-1} . The peaks at 1617 cm^{-1} and 1419 cm^{-1} are assigned to the imidazolium ring skeleton stretching in the $[\text{C}_{16}\text{mim}]\text{Br}$ molecules.^[17] In addition, the peak position at 1048 cm^{-1} is assigned to the C–N stretching vibration ($\nu_{\text{C-N}}$) mode of the imidazolium ring.^[18] From the FTIR spectra, it was found that there was the ionic liquid $[\text{C}_{16}\text{mim}]\text{Br}$ on the surface of the Cu polyhedron-pattern nanostructures. $[\text{C}_{16}\text{mim}]\text{Br}$ could not easily be removed from the surface of Cu polyhedron-pattern nanostructures by distilled water and absolute ethanol. These peaks are shifted slightly toward higher wavenumbers (2855 , 2925 , 1569 , 1467 , and 1000 cm^{-1}). This result suggests that there were chemical forces of interaction between the ionic liquid $[\text{C}_{16}\text{mim}]\text{Br}$ and the copper nanoparticles, which might have prevented the aggregation of crystallites and controlled the growth of Cu crystals. The as-prepared copper nanomaterials under different conditions were preserved at room temperature. It was found that the color of Cu synthesized in the absence of ionic liquid $[\text{C}_{16}\text{mim}]\text{Br}$ changed from red to black (the surface of Cu might be oxidized to CuO). However, the color of Cu polyhedron-pattern nanostructures did not change. Cu polyhedron-pattern nanostructures exhibited long-term thermal stability when $[\text{C}_{16}\text{mim}]\text{Br}$ adhered to the Cu surface. Ionic liquids, in particular imidazolium-

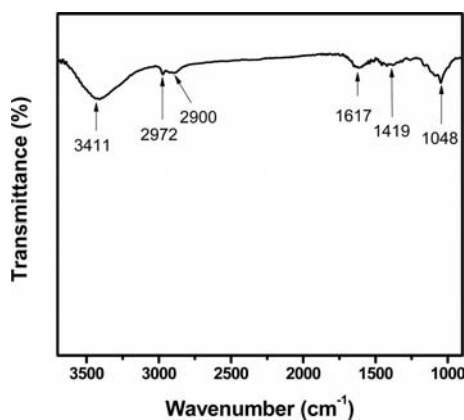


Figure 3. Typical FTIR spectrum of Cu polyhedron-pattern nanostructures.

based ILs, could stabilize metal nanoparticles on the basis of their high ionic charge, high polarity, high dielectric constant, and supramolecular network.^[13a,13b,13k]

2.4. UV/Vis Diffuse Reflectance Spectroscopy

The optical properties of Cu nanomaterials were measured by UV/Vis diffuse reflectance spectroscopy. Figure 4 shows the UV/Vis diffuse reflectance spectrum of Cu polyhedron-pattern nanostructures, as compared with that of Cu samples synthesized without ionic liquid. Both samples show a great increase in absorption at wavelengths lower than about 660 nm as a result of the band gap transition. This UV/Vis investigation indicates that the Cu nanoparticles absorb in the visible region. Consequently, they could be useful in the investigation of various optical phenomena, as novel supported photocatalysts, or as candidates for photonic crystals.^[19] Furthermore, a notable blueshift of the absorption of the Cu polyhedron-pattern nanostructures at the absorption edge is observed. The shift might be caused by a decrease in the size of Cu polyhedron-pattern nanostructures. It is well-known that the band gap energy of semiconductor nanoparticles increases with the decrease in size. The absorption peak shifted to a short wavelength. It was further confirmed that Cu polyhedron-pattern nanostructures synthesized with ionic liquid $[\text{C}_{16}\text{mim}]\text{Br}$ had smaller size, and this result was consistent with TEM results.

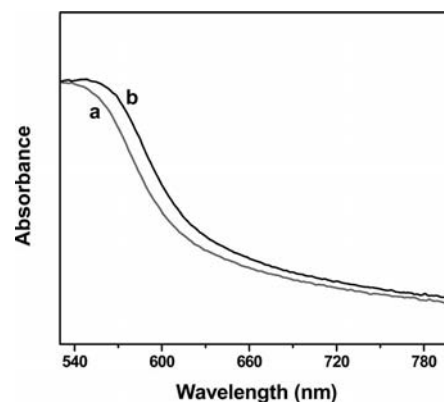


Figure 4. UV/Vis diffuse reflectance spectrum of as-prepared Cu samples: (a) in the presence of $[\text{C}_{16}\text{mim}]\text{Br}$ ionic liquid, (b) in the absence of $[\text{C}_{16}\text{mim}]\text{Br}$ ionic liquid.

2.5. Electrochemical Determination of Glucose without Enzyme

The electrocatalytic performance of electrodes modified with the Cu samples toward the oxidation of glucose in alkaline solution was investigated by cyclic voltammetry. In order to facilitate the following description, electrodes modified with Cu polyhedron-pattern nanostructures and Cu samples synthesized without ionic liquid are called Nafion/Cu^I/GC and Nafion/Cu^{II}/GC, respectively. Figure 5A shows cyclic voltammograms of Nafion/Cu^I/GC in the absence (curve a) and presence (curve b) of 5.0 mM glu-

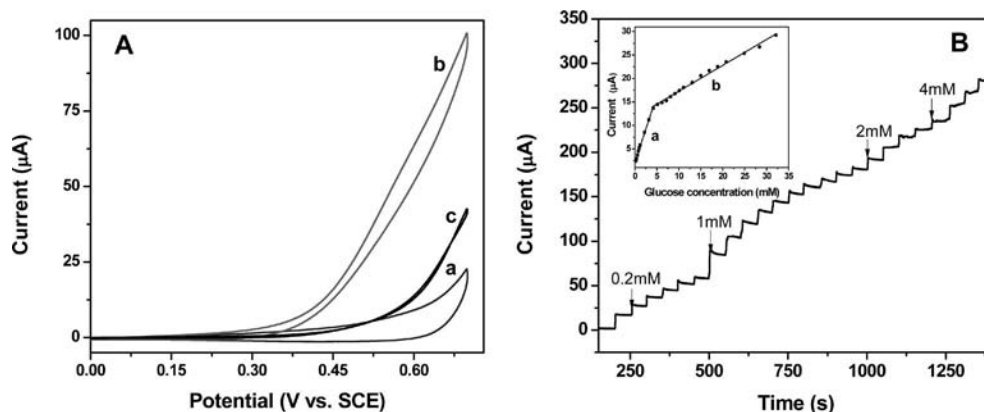


Figure 5. A: Cyclic voltammograms of Nafion/Cu^I/GC (a and b) and Nafion/Cu^{II}/GC in the absence (a) and presence (b and c) of 5.0 mM glucose in 0.10 M NaOH. Scan rate: 50 mV s⁻¹. B: Amperometric current vs. time curve for the detection of glucose at Nafion/Cu^I/GC. Glucose was injected into the stirred 0.10 M NaOH solution at regular intervals. The potential of the electrode was maintained at 0.50 V. The inset shows the corresponding calibration plot.

cose at a scan rate of 50 mV s⁻¹ in 0.10 M NaOH. With the addition of 5.0 mM glucose, the oxidative current significantly increased in the potential range 0.25–0.70 V, corresponding to the irreversible oxidation of glucose. This dramatic increase in the current indicates the significant catalytic activity of Nafion/Cu^I/GC toward glucose. As for Nafion/Cu^{II}/GC, an increase in the current signal was observed in the potential range 0.35–0.70 V (Figure 5A curve c). However, the oxidative current with Nafion/Cu^I/GC was about ten times that with Nafion/Cu^{II}/GC. It can be seen that Nafion/Cu^I/GC exhibits higher electrocatalytic performance than Nafion/Cu^{II}/GC. The data for Nafion/Cu^I/GC revealed high catalytic activity, which could be attributed to the fact that Cu polyhedron-pattern nanostructures have greatly increased electrocatalytically active area. Simultaneously, the [C₁₆mim]Br ionic liquid on the surface of the Cu polyhedron-pattern nanostructures had a significant impact on the electrocatalytic activity of Cu nanomaterials, because of the high ionic conductivity of the ionic liquid, which can accelerate electron transfer.^[20]

Constant-potential amperometry was further used to evaluate the performance of Nafion/Cu^I/GC. In the present investigation, the performance of Nafion/Cu^I/GC towards the detection of glucose was tested by recording the amperometric response (Figure 5B). The inset in Figure 5B shows that the plot of current (μA) vs. glucose concentration (mM) consists of two linear segments with different slopes (slopes: 2.1064 μA mM⁻¹ for the first linear segment and 11.7629 μA mM⁻¹ for the second linear segment), corresponding to two different ranges of substrate concentration (0.2 to 4.2 mM for the first linear segment; 4.2 to 32.1 mM for the second linear segment). The linear equations are: curve a: $y = 2.1064 + 2.8364x$ ($R = 0.9947$), and curve b: $y = 11.7629 + 0.5514x$ ($R = 0.9937$). The detection limit for glucose in the lower-range region was found to be 0.07 mM ($S/N = 3$). Uric acid (UA) and ascorbic acid (AA) in biological samples get easily oxidized at a lower positive potential than that of glucose, and consequently these biomolecules interfere with the detection of glucose.^[21] Therefore the interference tests

of the glucose sensors were carried out in 0.10 M NaOH by adding 2 mM glucose, followed with successive additions of 0.10 mM AA and 0.10 mM UA (Figure S1). Nafion/Cu^I/GC successfully detected the glucose in the presence of AA and UA, demonstrating almost negligible interference from AA and UA. Those results showed that Nafion/Cu^I/GC exhibited high sensitivity and selectivity to glucose.

3. Conclusion

In summary, Cu polyhedron-pattern nanostructures were prepared in the presence of ionic liquid [C₁₆mim]Br under solvothermal conditions. The nanomaterials synthesized with this method show good nanocrystallinity, stability, and small size. During the reaction process, the ionic liquid played an important role in controlling the morphology and size of Cu polyhedron-pattern nanostructures. The results of FTIR spectroscopic analysis indicated that there was the ionic liquid [C₁₆mim]Br on the surface of the Cu polyhedron-pattern nanostructures. Cu polyhedron-pattern nanostructures have better thermal stability in air than Cu samples synthesized without ionic liquid at room temperature. In addition, electrochemical studies revealed that Nafion/Cu^I/GC exhibits higher electrocatalytic performance than Nafion/Cu^{II}/GC. Simultaneously, [C₁₆mim]Br ionic liquid on the surface of the Cu polyhedron-pattern nanostructures has a significant impact on the electrocatalytic activity of Cu polyhedron-pattern nanostructures. Thus, electrodes modified with the Cu polyhedron-pattern nanostructures show promise for the future development of non-enzymatic glucose sensors.

4. Experimental Section

4.1. Materials and Sample Preparation: All chemicals were used as purchased, without further purification. Ionic liquid 1-hexadecyl-3-methylimidazolium bromide ([C₁₆mim]Br) was purchased from Shanghai Cheng Jie Chemical Co. LTD.

4.2. Preparation of the Cu Polyhedron-Pattern Nanostructures: In a typical procedure, CuCl₂·2H₂O (0.2728 g) and ionic liquid

[C₁₆mim]Br (2 g) were dissolved in EG solvent (20 mL) to form a homogeneous solution. Then, aqueous NaOH (1.28 mL, 5 M) was added dropwise into the above solution with vigorous stirring for 30 min. The molar ratio of CuCl₂·2H₂O to NaOH was 1:4. The solution was then transferred into a 25 mL Teflon-lined autoclave up to 80% of the total volume. The autoclave was heated at 160 °C for 48 h and cooled down to room temperature. The final product was separated by centrifugation, washed with distilled water and absolute ethanol four times, and dried under vacuum at 50 °C for 12 h before characterization. For comparison, Cu samples were also prepared by the same procedure but without the addition of ionic liquid.

4.3. Characterization: X-ray powder diffraction (XRD) analysis was carried out with a Bruker D8 diffractometer with high-intensity Cu-K_α ($\lambda = 1.54 \text{ \AA}$) in the 2θ range from 30° to 80°. High-resolution TEM (HRTEM) images were taken with a JEOL 2100 transmission electron microscope operated at 200 kV. The samples used for TEM were prepared by dispersing some product in ethanol, then placing a drop of the solution onto a copper grid and letting the ethanol evaporate slowly in air. FTIR spectrum was performed with a Nicolet FTIR spectrophotometer (Nexus 470, Thermo Electron Corporation) using KBr disks at room temperature. UV/Vis diffuse reflectance spectroscopy was recorded with a UV-2450 spectrophotometer (Shimadzu Corporation, Japan).

4.4. Measurement of Electrocatalytic Activity: Electrochemical measurements were performed by using a CHI 660B electrochemical workstation. A three-electrode system was employed with a glassy carbon (GC) electrode as the working electrode, a Pt wire as the auxiliary electrode, and an Ag/AgCl (3.0 M KCl) electrode as the reference electrode. The working electrode was prepared by following a literature procedure:^[22] as-synthesized Cu samples (1.0 mg) were dispersed in absolute ethanol (0.10 mL). The mixture was ultrasonicated for 10 min. Then, GC electrodes were modified by the ultrasonicated mixture (5 μ L) and dried in air. And then, a Nafion ethanol solution (5.0 μ L, 1%, V/V) was added dropwise onto the surface of the Cu/GC electrode. CV experiments were carried out with a scan rate of 50 mV s⁻¹ using a NaOH solution (0.10 mM) as the supporting electrolyte. Amperometric measurements were executed by a steady-state method in a NaOH solution (0.10 mM) under magnetic stirring, and the potential was set at 0.50 V.

Supporting Information (see footnote on the first page of this article): Current–time response of Nafion/Cu/GC electrode in 0.1 M NaOH at 0.50 V to injection of 2 mM glucose, 0.1 mM ascorbic acid, 0.1 mM uric acid.

Acknowledgments

This work was financially supported by the National Nature Science Foundation of China (No. 20876071, 21076099, and 21075054) and Jiangsu University Scientific Research Funding (No. 04JGD044).

- [1] A. S. Razavi, I. K. Snook, A. S. Barnard, *J. Mater. Chem.* **2010**, 20, 416–421.
- [2] C. L. Kitchens, C. B. Roberts, *Ind. Eng. Chem. Res.* **2004**, 43, 6070–6081.
- [3] L. P. Yu, H. J. Sun, J. He, D. H. Wang, X. B. Jin, X. H. Hu, G. Z. Chen, *Electrochem. Commun.* **2007**, 9, 1374–1381.
- [4] X. L. Ren, D. Chen, F. Q. Tang, *J. Phys. Chem. B* **2005**, 109, 15803–15807.
- [5] S. Kapoor, D. K. Palit, T. Mukherjee, *Chem. Phys. Lett.* **2002**, 355, 383–387.
- [6] R. V. Kumar, Y. Mastai, Y. Diamant, A. Gedanken, *J. Mater. Chem.* **2001**, 11, 1209–1213.
- [7] J. Wang, H. C. Huang, S. V. Kesapragada, D. Gall, *Nano Lett.* **2005**, 5, 2505–2508.
- [8] X. N. Cheng, X. F. Zhang, H. B. Yin, A. L. Wang, Y. Q. Xu, *Appl. Surf. Sci.* **2006**, 253, 2727–2732.
- [9] S. H. Johnson, C. L. Johnson, S. J. May, S. Hirsch, M. W. Cole, J. E. Spanier, *J. Mater. Chem.* **2010**, 20, 439–443.
- [10] X. Y. Song, S. X. Sun, W. M. Zhang, Z. L. Yin, *J. Colloid Interface Sci.* **2004**, 273, 463–469.
- [11] a) R. E. Morris, *Chem. Commun.* **2009**, 2990–2998; b) Z. J. Lin, A. M. Z. Slawin, R. E. Morris, *J. Am. Chem. Soc.* **2007**, 129, 4880–4881; c) E. R. Parnham, R. E. Morris, *J. Am. Chem. Soc.* **2006**, 128, 2204–2205.
- [12] a) Z. Ma, J. H. Yu, S. Dai, *Adv. Mater.* **2010**, 22, 261–285; b) T. Alammari, A. Birkner, A. Mudring, *Eur. J. Inorg. Chem.* **2009**, 2765–2768.
- [13] a) J. Dupont, J. D. Scholten, *Chem. Soc. Rev.* **2010**, 39, 1780–1804; b) M. A. Neouze, *J. Mater. Chem.* **2010**, 20, 9593–9607; c) X. T. Bai, X. W. Li, L. Q. Zheng, *Langmuir* **2010**, 26, 12209–12214; d) X. T. Bai, Y. N. Gao, H. G. Liu, L. Q. Zheng, *J. Phys. Chem. C* **2009**, 113, 17730–17736; e) Y. Gao, A. Voigt, M. Zhou, K. Sundmacher, *Eur. J. Inorg. Chem.* **2008**, 3769–3775; f) Z. H. Li, Z. M. Liu, J. L. Zhang, B. X. Han, J. M. Du, Y. N. Gao, T. Jiang, *J. Phys. Chem. B* **2005**, 109, 14445–14448; g) P. Singh, S. Kumar, A. Katyal, R. Kalra, R. Chandra, *Mater. Lett.* **2008**, 62, 4164–4166; h) E. Redel, J. Krämer, R. Thomann, C. Janiak, *J. Organomet. Chem.* **2009**, 694, 1069–1075; i) E. Redel, R. Thomann, C. Janiak, *Chem. Commun.* **2008**, 1789–1791; j) E. Redel, R. Thomann, C. Janiak, *Inorg. Chem.* **2008**, 47, 14–16; k) E. Redel, M. Walter, R. Thomann, C. Vollmer, L. Hussein, H. Scherer, M. Krüger, C. Janiak, *Chem. Eur. J.* **2009**, 15, 10047–10059.
- [14] E. Redel, M. Walter, R. Thomann, L. Hussein, M. Krüger, C. Janiak, *Chem. Commun.* **2010**, 46, 1159–1161.
- [15] a) K. Richter, A. Birkner, A. Mudring, *Angew. Chem.* **2010**, 122, 2481; *Angew. Chem. Int. Ed.* **2010**, 49, 2431–2435; b) J. Kim, S. W. Kang, S. H. Mun, Y. S. Kang, *Ind. Eng. Chem. Res.* **2009**, 48, 7437–7441; c) D. Raut, K. Wankhede, V. Vaidya, S. Bhilare, N. Darwatkar, A. Deorukhkar, G. Trivedi, M. Salunkhe, *Catal. Commun.* **2009**, 10, 1240–1243; d) M. Brettholle, O. Höfft, L. Klarhöfer, S. Mathes, W. Maus-Friedrichs, S. Z. El Abedin, S. Krischok, J. Janek, F. Endres, *Phys. Chem. Chem. Phys.* **2010**, 12, 1750–1755; e) L. Zhu, Y. Chen, Y. Sun, Y. Cui, M. Liang, J. Zhao, N. Li, *Cryst. Res. Technol.* **2010**, 45, 398–404; f) P. Singh, A. Katyal, R. Kalra, R. Chandra, *Tetrahedron Lett.* **2008**, 49, 727–730; g) P. Singh, A. Katyal, R. Kalra, R. Chandra, *Catal. Commun.* **2008**, 9, 1618–1623.
- [16] K. Nakamoto, *Infrared Spectra of Inorganic and Coordination Compounds*, Wiley, New York, **1986**, fourth ed.
- [17] H. W. Che, S. H. Han, W. G. Hou, A. Liu, X. J. Yu, Y. Y. Sun, S. S. Wang, *Microporous Mesoporous Mater.* **2010**, 130, 1–6.
- [18] Y. Zhou, J. H. Schattka, M. Antonietti, *Nano Lett.* **2004**, 4, 477–481.
- [19] Y. Liu, Y. Chu, Y. J. Zhou, L. H. Dong, L. L. Li, M. Y. Li, *Adv. Funct. Mater.* **2007**, 17, 933–938.
- [20] X. Q. Li, R. J. Zhao, Y. Wang, X. Y. Sun, W. Sun, C. Z. Zhao, K. Jiao, *Electrochim. Acta* **2010**, 55, 2173–2178.
- [21] T. G. S. Babu, T. Ramachandran, B. Nair, *Microchim. Acta* **2010**, 169, 49–55.
- [22] G. F. Wang, Y. Wei, W. Zhang, X. J. Zhang, B. Fang, L. Wang, *Microchim. Acta* **2010**, 168, 87–92.

Received: November 1, 2010

Published Online: February 21, 2011